The Microwave Spectrum of 2,6-Difluoropyridine

I. Assignment and Complete Structure by DRM Spectroscopy

Otto L. Stiefvater

School of Physical and Molecular Sciences, University College of North Wales
Bangor, Gwynedd, U.K.

(Z. Naturforsch. **30 a**, 1765–1775 [1975]; received October 6, 1975)

Double resonance modulated (DRM) microwave spectroscopy has been used for the assignment of the rotation spectrum of 2,6-difluoropyridine, and for the study of 10 non-equivalent isotopic forms of this compound. All ^{13}C and ^{15}N spectra were observed in their natural abundances. From these data the complete structure of 2,6-difluoropyridine has been derived. The geometry of the ring was determined independently in two reference frames.

Bond distances (in Å, uncertainties 0.001 Å) an bond angles (in degrees, uncertainty 0.1°) are as follows: N(1)–C(2/6) = 1.3168, C(2/6)–C(3/5) = 1.3767, C(3/5)–C(4) = 1.3941, C(2/6)–F(2/6) = 1.347, C(3/5)–H(3/5) = 1.0795, C(4)–H(4) = 1.0822. Angles: C(2)N(1)C(6) = 115.0, N(1)C(2/6)C(3/5) = 126.5, C(2/6)C(3/5)C(4) = 116.1, C(3)C(4)C(5) = 119.8, N(1)C(2/6)F(2/6) = 114.7, C(2/6)C(3/5)H(3/5) = 120.8 and C(3/5)C(4)H(4) = 120.1. These data represent the first quantitative experimental verification of previously postulated distortions of the pyridine ring under substitution.

I. Introduction

Concurrently with the thorough investigation of the rotation spectrum of pyridine [1] there have been a number of microwave studies of substituted pyridines: The barriers to internal rotation have been studied in 4- and 2-methylpyridine [2a, b]. The effects due to inversion of the NH_2-group have been observed in 2-aminopyridine [2c], and similar studies have been carried out on 3- and 4-aminopyridine [2d]. Quadrupole coupling constants have been determined for 2-fluoro-, 2-chloro- and 2- and 4-bromopyridine [2e–g], for pentafluoropyridine [2h] and the two methylpyridines [2a, b]. The electric dipole moment has been measured for pyridine-N-oxide [2i] and the other compounds mentioned, with the exception of the chloro- and bromopyridines [2f, g]. The microwave spectrum of 2-cyanopyridine [2j] has also been assigned.

While these studies have yielded valuable information on the force field and the electron distribution within these molecules, no quantitative data have been obtained concerning the geometry of the ring in substituted pyridines. In fact, for all twelve compounds studied so far [2], the ring structure was assumed as in pyridine. In several cases [2e, h, j] this assumption led to serious discrepancies however between the observed rotational constants on the one hand, and reasonable bond lengths between the ring and the substituent on the other hand. Hence, analogous ring distortions as in corresponding benzene derivatives [3] were invoked [2k] also for substituted pyridines. A quantitative examination of these effects by traditional microwave techniques remained apparently unfeasible.

Despite this somewhat discouraging record, we took up a suggestion [4a] to derive structural information on 2,6-difluoropyridine (2,6-DFP), especially since we were confident that we could determine the complete structure, so that the first quantitative data concerning the distortion of the ring and the C–F bond length in a substituted pyridine would be obtained. While Stark effect modulated (SEM) microwave spectroscopy could hardly attack such a task without the preparation of expensive isotopic species, recent developments from this laboratory [5] have shown that these problems can often be by-passed in double resonance modulated (DRM) spectroscopy [6]. This experimental approach offers not only sufficient sensitivity for the observation of rare isotopic species (e.g. ^{13}C, ^{15}N, ^{18}O) in their natural abundances, but also provides the required molecular selectivity for almost effortless analysis of the spectra from partially enriched or natural mixtures of isotopic species. In view of the studies [2] mentioned above, 2,6-DFP seemed a good example to demonstrate the power of the DRM technique once more.

As a proper reflection of the sequence of the work on 2,6-DFP we report in this present Part I

Reprint requests to Otto L. Stiefvater, School of Physical and Molecular Sciences, University College of North Wales, *Bangor, Gwynedd*, U.K.

the assignment of the spectrum and the complete structure, as obtained by DRM spectroscopy alone. The subsequent study by traditional techniques of DRM assigned (Sect. III-B-1) vibrational satellite spectra, and the determination of the nuclear quadrupole coupling constants and of the molecular dipole moment of 2,6-DFP will be the subjects of Part II.

II. Experimental

1. Samples

The sample of 2,6-DFP was kindly provided by Dr. J. Ladd and Mr. S. Lui (University of Salford, U.K.) together with a 90% enriched sample of 2,6-DFP-d_4 and a 20% enriched sample of the perdeutero compound [4b]. Only a very small sample of the perdeutero form was available, and re-protonation of this sample at the 4-position was therefore not feasible (see Section IV). Isotopic forms involving ^{13}C and ^{15}N (see Table 2) were studied in their natural abundances.

2. Instrumental

Apart from a cursory survey of the K-band spectrum (18 – 26 GHz) in a conventional SEM spectrometer, all experimental work was conducted by DRM spectroscopy. A description of the instrument and the mode of operation has been given in the literature [6b, c]. After the spectrum had been assigned (Sect. III-A-3) the frequency area for investigation was restricted to pump frequencies between 22 GHz and 26 GHz and to signal frequencies between 28 GHz and 35 GHz. The pump klystron used for all experiments was an OKI, type 24 V 10 A, with a power output of $\sim$200 mW. Measurements were carried out at room temperature and at a sample pressure of $\sim$20 mTorr.

III. Results

A) Normal Species

1. Spectrum

2,6-DFP is a prolate asymmetric rotor ($\varkappa = -.48272$) with the dipole moment along the axis of the intermediate moment of inertia (C_{2v} symmetry axis). As the molecule is comparatively heavy, its spectrum is dominated by several series of Q-branch transitions which extend up to $J = 35$. Small hyperfine splittings due to the quadrupolar ^{14}N nucleus are noticeable on many transitions, particularly for $J < 15$. There are several low frequency vibrations [7] which give rise to detectable satellites in the rotation spectrum.

2. Molecular Models

As in all previous studies on substituted pyridines [2], the prediction of the spectrum had to be based on the more than questionable assumption that the structure of the pyridine ring would not be affected by substitution of fluorine in the 2- and 6-position. This left only the CF bond length and the NCF angle as adjustable model parameters. Accordingly, the normal and the DRM spectrum were calculated for a series of models in which the CF bond length was varied from 1.32 Å [2e] to 1.35 Å [3b], while the NCF angle was allowed to deviate from 120° by $\pm 5°$. From these calculations the frequencies of most strong Q-branch transitions were seen to be rather sensitive to the assumed structure, and therefore not very promising for the assignment of the spectrum. The low-J R-branch transitions appeared equally unsuitable because of their small intensity, their expected hyperfine splitting, and the likelihood that such transitions might be "buried" under the numerous strong Q-branches or their satellites. For these reasons, an assignment of the spectrum by SEM spectroscopy was not attempted.

3. Assignment by DRM Spectroscopy

From the model calculations on 2,6-DFP the ground state spectrum alone could be expected to give rise to $\sim$110 signals within the frequency area specified in Section II-2, if J-values up to $J = 35$ and an intensity variation by a factor 30 were considered. Inclusion of signals due to excited vibration states easily doubles this figure. Naturally, the uncertainty in the position of the Q-branch transitions also exists in the DRM spectrum and, while connections between such transitions were readily observed in an exploratory experiment, rotational assignments of these signals could not be infered with any degree of confidence. Hence, in order to avoid the somewhat "pedestrian" procedure of trial assignments followed by repredictions and, hopefully, eventual success, we chose a different route to the assignment which was sign-posted by the following considerations.

The most striking feature of the predicted DRM spectra of 2,6-DFP was the occurrence of two Q-branch pump transitions, each of which shares a

Table 1. Preselected key DR-connections of 2,6-difluoropyridine.

Transitions	Rel. Int. [a]	Predicted frequency	Estimated uncertainty [b]	Transitions	Rel. Int. [a]	Line-shape	Predicted frequency	Estimated uncertainty [b]
Pump				Signal				
Set A								
$\nu_p^A = 11_{0,11} - 11_{1,10}$	18	25523	±190	$\nu_{S1}^A = 10_{1,10} - 11_{0,11}$	87	I	28954	±200
				$\nu_{S2}^A = 10_{2,9} - 11_{1,10}$	68	II	31398	±220
				$\nu_{S3}^A = 11_{0,11} - 12_{1,12}$	96	II	31475	±220
				$\nu_{S4}^A = 11_{1,10} - 12_{2,11}$	77	I	34063	±230
Set B								
$\nu_p^B = 11_{1,11} - 11_{2,10}$	18	25588	±190	$\nu_{S1}^B = 10_{0,11} - 11_{1,11}$	87	I	28960	±200
				$\nu_{S2}^B = 11_{1,11} - 12_{0,12}$	96	II	31473	±220
				$\nu_{S3}^B = 10_{1,9} - 11_{2,10}$	68	II	31610	±230
				$\nu_{S4}^B = 11_{2,10} - 12_{1,11}$	77	I	33967	±240

[a] in arbitrary units. [b] The upper frequency limits correspond to a model CF-bond length of 1.32 Å, the lower limits to CF = 1.35 Å.

level with four R-branch signal transitions (see Table 1). The intensity of the pump transitions is only ~0.1 of the strongest transitions in the spectrum, but their frequencies were found insensitive to the assumed structure and appeared predictable to within ±200 MHz for the model range specified in Section 2. Their separation could be expected to be 40 – 60 MHz. The eight R-branch signal transitions are of medium intensity and appeared predictable to within ±250 MHz. Moreover, it was noted that the transition ν_{S1}^A (see Table 1) and the transition ν_{S1}^B should occur within less than 10 MHz of each other, and that the transition ν_{S3}^A should not be separated by more than 5 MHz from the transition ν_{S2}^B.

While these considerations involved only the frequencies of DR-connected transitions, the most stringent criterion and, hence, the most useful clues towards the assignment arose from the lineshape [6d] of the expected DRM signals. Consideration of the disposition of the energy levels revealed that the signals 1 and 4 of each set belong to the more frequent type I (common level intermediate in energy) whereas signals 2 and 3 belong to the rarer type II (common level energetically highest or lowest). Accordingly, if one of the four more distinctive type II signals could be found in the predicted frequency area, there would have to be a second type II signal either within ~70 MHz if the pump transition was $\nu_p{}^A = 11_{0,11} - 11_{1,10}$, or within ~140 MHz if the pump transition happened to be $\nu_p{}^B = 11_{1,11} - 11_{2,10}$.

With these aspects in mind, we began the experiment to assign 2,6-DFP with a double search [6b, c] for type II signals between $\nu_p \sim 25.5$ GHz and $\nu_S \sim 31.5$ GHz (compare Table 1) and, by keeping either the signal or the pump frequency fixed in subsequent steps (see below) of this experiment, we were able to deduce the complete assignment of 10 Q- and 12 R-branch transitions. Thus, 22 transitions were available for the first attempt to fit the spectrum. The result of the least squares fit [8] confirmed not only each individual assignment, but also gave rotational constants which were accurate enough to make the DRM identification of transitions up to $J = 33$ straightforward.

Details of the experiment to assign 2,6-DFP may best be followed with the help of the "pictorial" double resonance map [6b, c] of Figure 1. For clarity, we have separated in this figure the two families of signals in accord with Table 1, although both sets occur in the same area and are, therefore, intermingled. Signals associated with set A of Table 1 (first row in Fig. 1) are shown in the upper half with the zero-pump lines [6] pointing upwards, and those linked with set B (fifth row in Fig. 1) are assembled in the lower half of this figure with the zero-pump lines pointing downwards.

Step 0: Double search (ν_p and ν_S variable, unknown)

Beginning with the modulated pump radiation at ~25.55 GHz, we shifted the pump frequency in steps of ~60 MHz and searched the signal range from 31.3 – 31.7 GHz for each setting of the pump klystron. The third scan yielded a signal with type II lineshape near 31,544 MHz which, after exact resonance had been established, identified the pump frequency as 25,748.0 MHz and the signal frequency as 31,544.9 MHz. The expected companion signal (same pump frequency) with type II lineshape was found at 31,583.6 MHz. The separation between these two signals and the fact that the pump transi-

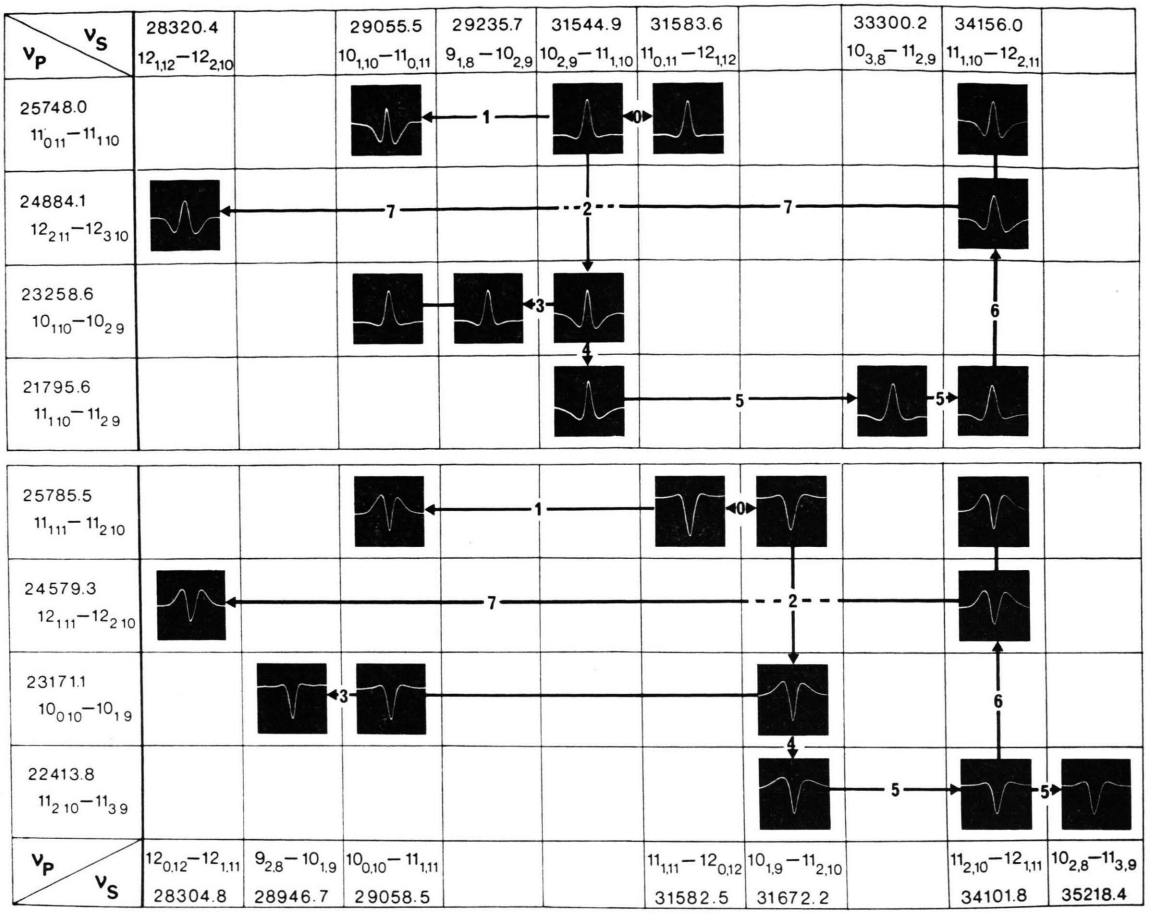

Fig. 1. Transitions and signals used in the DRM assignment of 2,6-difluoropyridine ("Pictorial" double resonance map).

Table 2. Rotational parameters of the normal

		I	II	III	IV	V
1	Isotopic species	Normal	^{15}N (1)	^{13}C (2/6)	^{13}C (3/5)	^{13}C (4)
2	Signal transitions in fit	23 R & 38 Q	8 R & 20 Q	14 R & 27 Q	15 R & 29 Q	11 R & 32 Q
3	Range of J-values	9−33 & 12−27	9−12 & 13−29	9−14 & 12−29	4−23 & 12−29	9−18 & 11−30
4	A	3747.701 (24) [a]	3723.250 (32)	3746.188 (33)	3712.639 (38)	3656.646 (33)
5	B	1905.832 (12)	1905.911 (9)	1897.056 (9)	1895.389 (11)	1905.848 (11)
6	C } in MHz	1263.253 (11)	1260.498 (8)	1259.222 (6)	1254.677 (9)	1252.740 (7)
7	τ_{aaaa}	−2.56 (30)	−2.6 (12)	−3.1 (15)	−2.0 (15)	−1.6 (13)
8	τ_{bbbb}	− .49 (6)	− .49 ass.	− .48 (6)	− .45 (6)	− .45 (6)
9	τ_{aabb} } in kHz	.35 (16)	.35 ass.	.35 ass.	.35 ass.	.35 ass.
10	τ_{abab}	− .47 (9)	− .47 (14)	− .36 (12)	− .52 (14)	− .54 (12)
11	I_a	134.8496 (8)	135.7352 (11)	134.9041 (12)	136.1231 (14)	138.2075 (14)
12	I_b	265.1734 (18)	265.1625 (12)	266.4002 (12)	266.6345 (15)	265.1712 (15)
13	I_c } in μÅ²	400.0593 (31)	400.9335 (24)	401.3399 (17)	402.7939 (27)	403.4166 (24)
14	I.D.	.0363 (40)	0.359 (29)	.0356 (26)	.0361 (33)	.0379 (30)

[a] Uncertainties are three times the standard deviation, and given in units of the last digit quoted.

tion had been approached from below suggested strongly that the pump transition was the $11_{0.11} - 11_{1.10}$, forcing the assignments 31,544.9 MHz = $10_{2.9} - 11_{1.10}$ and 31,583.6 MHz = $11_{0.11} - 12_{1.12}$. If this conclusion was correct, the $11_{1.11} - 12_{0.12}$ had to occur close to 31,583 MHz as soon as the pump frequency was increased by some 50 MHz. This was indeed the case as a pump frequency of 25,785.5 MHz = $11_{1.11} - 11_{2.10}$ gave rise to the expected type II signal at 31,582.5 MHz = $11_{1.11} - 12_{0.12}$, with the required companion signal at 31,672.2 MHz = $10_{1.9} - 11_{2.10}$. For further support of these assignments we continued as follows.

Step 1: (ν_p = constant, known)

With the pump frequency fixed at 25,785.5 MHz the signal frequency was tuned down towards 29.0 GHz to yield the transition $10_{0.11} - 11_{1.11}$ with the predicted type I lineshape at 29,058.5 MHz. Readjustment of ν_p to the known value of 25,748.0 MHz gave readily $10_{1.10} - 11_{0.11}$ = 29,055.5 MHz.

Step 2: (ν_S = constant, known)

After return to the initial signal at 31,544.9 MHz the pump frequency was brought down into the predicted range for the transition $10_{1.10} - 10_{2.9}$ and then slowly tuned until the signal at 31,544.9 MHz re-appeared with the expected type I lineshape for ν_p = 23,258.6 MHz. Similarly, the re-appearance of the signal at 31,672.2 MHz revealed the frequency of the pump transition $10_{0.10} - 10_{1.9}$ as 23,171.1 MHz.

Step 3: (ν_p = constant, known)

With the pump transitions identified in step 2 the assignment of the transitions $9_{1.8} - 10_{2.9}$ = 29,325.7 MHz and $9_{2.8} - 10_{1.9}$ = 28,946.7 MHz was unequivocal, since they both showed the required type II lineshape for the same respective pump frequencies as the signals at 29,055.5 MHz and 29,058.6 MHz which had been identified in step 1.

Step 4: (ν_S = constant, known)

After return of the signal frequency to 31,672.2 MHz the pump frequency was shifted to the predicted range for the transition $11_{2.10} - 11_{3.9}$ and then slowly tuned until the $10_{1.9} - 11_{2.10}$ was at resonance again, indicating that the desired $J = 11$ pump transition occurred at 22,413.8 MHz. In the same manner, the transition $11_{1.10} - 11_{2.9}$ = 21,795.6 MHz was identified by observation of the resonance of the known signal transition at 31,544.9 MHz.

Step 5: (ν_p = constant, known)

With the same procedure as described in steps 1 and 3 the transitions $10_{3.8} - 11_{2.9}$ = 33,300.2 MHz and $11_{1.10} - 12_{2.11}$ = 34,156.0 MHz were identified next (ν_p = 21,795.6 MHz from step 4), as well as the transitions $11_{2.10} - 12_{1.11}$ = 34,101.8 MHz and $10_{2.8} - 11_{3.9}$ = 35,218.4 MHz (ν_p = 22,413.8 MHz).

Step 6: (ν_S = constant, known)

Knowledge of the transitions $11_{2.10} - 12_{1.11}$ and $11_{1.10} - 12_{2.11}$ observed in step 5 as type II signals allowed the $J = 12$ pump transition to be located in

and isotopic forms of 2,6-difluoropyridine.

VI	VII	VIII	IX	X	XI
D(4)	D(4) $-^{15}$N(1)	D(4) $-^{13}$C(2/6)	D(4) $-^{13}$C(3/5)	D(4) $-^{13}$C(4)	D(3)–D(4)–D (5)
30 R & 30 Q	11 R & 20 Q	14 R & 35 Q	13 R & 33 Q	13 R & 32 Q	26 R & 40 Q
4–30 & 10–30	9–12 & 15–31	9–18 & 10–30	8–12 & 10–31	9–17 & 14–31	4–31 & 14–32
3525.486 (17)	3502.659 (33)	3523.834 (39)	3495.843 (28)	3447.011 (22)	3405.138 (9)
1905.810 (9)	1905.883 (9)	1897.041 (12)	1895.376 (9)	1905.836 (7)	1840.087 (5)
1236.965 (7)	1234.176 (5)	1233.062 (8)	1228.916 (6)	1227.167 (5)	1194.489 (5)
−1.99 (23)	−2.2 (12)	−1.7 (12)	−2.6 (9)	−2.3 (6)	−1.97 (16)
− .45 (5)	− .47 (7)	− .47 (7)	− .49 (6)	− .49 (4)	− .43 (3)
.37 (15)	.37 ass.	.37 ass.	.37 ass.	.37 ass.	.27 (8)
− .44 (10)	− .42 (12)	− .51 (11)	− .39 (9)	− .44 (6)	− .39 (5)
143.3493 (7)	144.2835 (14)	143.4165 (16)	144.5648 (12)	146.6128 (9)	148.4157 (4)
265.1765 (12)	265.1664 (13)	266.4023 (17)	266.6362 (12)	265.1729 (9)	274.6479 (7)
408.5612 (25)	409.4846 (17)	409.8544 (27)	411.2374 (19)	411.8233 (15)	423.0895 (16)
.0354 (30)	.0347 (26)	.0356 (33)	.0363 (25)	.0376 (19)	.0259 (19)

the manner described in step 2, since each one of these signals had to re-appear with a type I lineshape when the pump frequency coincided with the desired pump transition. This yielded $12_{2,11} - 12_{3,10} = 24{,}884.1$ MHz and $12_{1,11} - 12_{2,10} = 24{,}579.3$ MHz. To complete the two sets of signals as planned in Table 1, we confirmed on that occasion the connections $\nu_p{}^A \rightarrow \nu_{S4}^A = 25{,}748.0$ MHz $\rightarrow 34{,}156.0$ MHz and $\nu_p{}^B \rightarrow \nu_{S4}^B = 25{,}785.5$ MHz $\rightarrow 34{,}101.8$ MHz.

Step 7: (ν_p = constant, known)

Utilising the two pump transitions identified in step 6 we finally observed the first Q-branch signal transitions: $12_{1,12} - 12_{2,10} = 28{,}328.4$ MHz and $12_{0,12} - 12_{1,11} = 28{,}304.8$ MHz.

4. Rotation and Distortion Constants

The comparatively large weight of 2,6-DFP required a very accurate determination of the rotational constants if the moments of inertia were to be obtained with the usual accuracy of 0.001 μÅ^2. Since hyperfine splittings rendered the low J-transitions unsuitable to provide such accuracy, we bypassed the analysis of the quadrupole fine structure altogether, and concentrated on transitions with $J > 10$. Due to the unequivocal assignment afforded by DRM spectroscopy, over 100 transitions were readily identified, including over 40 R-branch lines with J-values up to $J = 33$. All transitions could be matched within experimental accuracy to a Hamiltonian [8] including forth order terms in the angular momenta. Final values of the rotational parameters were obtained from a least squares fit of 61 signal transitions [9]. The results are given in column I of Table 2.

B) Isotopic Species

1. Vibrational Satellites, Assessment of Sensitivity

In analogy to the approach which we have found expedient in previous structure determinations [5], the study of isotopic species spectra was preceeded by a brief investigation of vibrational satellites. Nine such spectra were easily identified by DRM methods [6e] and complete rotational assignments (Q- and R-branch) were obtained. Knowledge of these satellite spectra not only facilitated the later identification of isotopic species spectra, but also allowed an early assessment of the detectability of rare isotopic forms in natural abundance, in particular of the ^{15}N species (compare ref. 5 b, Section III,B). To this end, we followed a sequence of DRM signals [6e] associated with successive excitation of the lowest vibrational mode $\nu_{13} = 219$ cm^{-1} (7) up to the fifth excited state. This level, which could be expected to lie ~ 1100 cm^{-1} above the ground state, has a relative population (0.4%) which is comparable with the natural abundance of ^{15}N (0.36%). Hence, the intensity of its signals provided a good measure for the intensity of corresponding transitions of the ^{15}N spectrum. The detectability of all rare isotopic forms was thus ascertained prior to the structure determination. Subsequent results (Table 2 and Fig. 1) fully confirmed the soundness of this approach.

2. Sequence of Isotopic Analysis

The first isotopic species studied was the D(4) form (90% enriched sample), since this species fixes the furthest extension of 2,6-DFP along the b-direction (see Figure 3). The results allowed the C(4)-position to be estimated with reasonable confidence, and the ^{13}C(4) spectrum was then readily assigned. Next, the pyridine values [1e] for the C(4) – C(3/5) bond length and the angle C(3) C(4) C(5) were used in conjunction with the known position of C(4) to predict and identify the ^{13}C(3/5) spectrum. Knowledge of the coordinate of C(4) in 2,6-DFP together with the N – C(4) distance of pyridine also allowed the identification of the ^{15}N spectrum. The ^{13}C(2/6) spectrum occurs closest to the ground state transitions of the normal form and is therefore intermingled with vibrational satellites. Since these had been assigned beforehand (Sect. 1, above), no difficulties were encountered in completing the ring structure through the assignment of the ^{13}C(2/6) spectrum. All isotopic species pertaining to the ring itself were then studied for a second time with the D(4) species as parent molecule. Naturally, the previously established geometry of the ring was used to predict these spectra so that the spectroscopic work could be completed correspondingly quicker. The perdeuterated form (20% enriched) was studied last.

3. Rotational Parameters of Isotopic Species

The assignment of individual isotopic forms was accomplished by double searches [6b, c], and a detailed account of the transitions used will be given elsewhere [6f]. Rotational and distortion constants were derived as described for the ground state of the normal species (Sect. III-A-4, above). Except for deuterium forms, the distortion constant τ_{aabb} could

not be fixed with reasonable accuracy for the isotopic species and was therefore held fixed in the least squares fits. For reasons explained previously [6c] only signal transitions were included in the fits. Their numbers and the range of J-values investigated are included in Table 2, in which the rotational parameters of all isotopic species are collected.

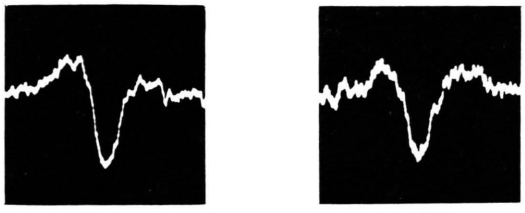

Fig. 2. Assessment of the relative intensity of the ^{15}N spectrum through an excited vibration state ($5\times v_1$), and a later observed signal of the ^{15}N species. Transitions (and relative intensities) are as follows:
$5\times v_1$: $\nu_p \sim 24425.0$ MHz $= 28_{9,19}-28_{10,18}$ (17.5),
$\nu_s = 31468.4$ MHz $= 28_{10,18}-28_{11,17}$ (14.7).
^{15}N: $\nu_p \sim 22291.3$ MHz $= 24_{8,16}-24_{9,15}$ (15.5),
$\nu_s = 30668.5$ MHz $= 24_{9,15}-24_{10,14}$ (12.7).

The absolute values of the rotational constants together with the relative intensities of transitions (Fig. 2) leave little doubt that all isotopic species spectra are correctly interpreted. The inertia defects (row 14 of Table 2), which for all but the per-deutero-species (column XI) coincide within limits of $\pm 4\%$, lend still further support for the correctness of the isotopic analysis. The large percentage decrease ($\sim 30\%$) of the inertia defect in the per-deutero-form parallels the findings in fluorobenzene [3b].

IV. Molecular Structure

With Kraitchman's equations [10a] for planar molecules the atomic coordinates of 2,6-DFP were calculated in the principal axis frame of the normal

Table 3. Structure calculations on 2,6-difluoropyridine.

		I Normal frame		II D(4)-frame		III Average r_S in normal frame		IV LSQ 2		r_S- LSQ 2
a)	*Coordinates*	*a*	*b*	*a*	*b*	*a*	*b*	*a*	*b*	
1	N(1)	—	.9435[30][a]	—	.9693[30]	—	.9437[3]	—	.9436	
2	C(2/6)	1.1102[2]	.2346[6]	1.1098[1]	.2613[3]	1.1100[2]	.2353[7]	1.1106	.2361	
3	C(3/5)	1.2060[1]	1.1378[1]	1.2055[3]	1.1121[3]	1.2058[3]	1.1376[2]	1.2063	1.1376	
4	C(4)	—	1.8373[1]	—	1.8111[2]	—	1.8368[5]	—	1.8368	
5	H(4)	—	2.9192[2]	—	2.8939[2]	—	2.9192[–]	—	2.9189	
6	H(3/5)	{2.1690	1.6251}	2.1690[7]	1.5998[7]	2.1690[7]	1.6251[7]	2.1694	1.6253	
7	F(2/6)[b]	2.2417[6][c]	.9667[13]	2.2420[6]	.9904[10]	2.2420[6]	.9659[8]	2.2428	.9654	
b)	*Bond lengths*									
8	N(1)–C(2/6)	1.3172[15]		1.3164[17]		1.3168[4]		1.3168(5)		0
9	C(2/6)–C(3/5)	1.3757[10]		1.3768[6]		1.3762[6]		1.3770(3)		−8
10	C(3/5)–C(4)	1.3942[1]		1.3935[4]		1.3938[4]		1.3943(5)		−5
11	C(4)–H(4)	1.0819[3]		1.0828[4]		1.0823[5]		1.0821(5)		+2
12	C(3/5)–H(3/5)	1.0793[5]		1.0799[7]		1.0796[3]		1.0795(3)		+1
13	C(2/6)–F(2/6)	1.3477[12]		1.3467[4]		1.3472[5]		1.3468(1)		+4
c)	*Angles*									
14	C(6)N(1)C(2)	114.88[18]		114.86[29]		114.90[5]		115.00(5)		−10
15	N(1)C(2)C(3)	126.55[9]		126.52[12]		126.54[2]		126.49(3)		+5
16	C(2)C(3)C(4)	116.12[2]		116.12[3]		116.12[0]		116.11(5)		+1
17	C(3)C(4)C(5)	119.77[1]		119.79[3]		119.78[1]		119.80(3)		−2
18	C(3)C(4)H(4)	120.11[1]		120.10[2]		120.11[1]		120.10(5)		+1
19	C(4)C(3)H(3)	123.04[6]		123.05[9]		123.05[1]		123.04(4)		+1
20	C(2)C(3)H(3)	120.84[6]		120.83[8]		120.83[1]		120.85(4)		−2
21	N(1)C(2)F(2)	114.53[5]		114.68[9]		114.61[3]		114.71(5)		−10
22	C(3)C(2)F(2)	118.92[9]		118.80[3]		118.85[7]		118.80(5)		+5
23	$I_a^{eff.}-I_a^{subst.}$ [d]	.0672 ≙ .05%		.2109 ≙ .15%		.1436 ≙ .11%		.1709 ≙ .13%		
24	$I_b^{eff.}-I_b^{subst.}$	.2654 ≙ .10%		.2654 ≙ .10%		.2320 ≙ .09%		.0370 ≙ .01%		

[a] Numbers in square brackets reflect the compatibility of the data, rather than uncertainties. Like statistical uncertainties (in round brackets) they are given in units of the last digit.
[b] These coordinates are *not* substitution values (see text).
[c] These values include an uncertainty of $\pm .05\%$ in the assumed difference (.10%) between the observed I_b and that expected for the substitution structure.
[d] in $\mu Å^2$.

form and of the d_4-species. As the changes ($\Delta I_{g=a,b,c}$) under substitution of two moments alone suffice for placing the substituted atom in the case of a planar structure, *all* calculations were carried out with each of the three possible combinations of ΔI_g-values. The averaged results for the coordinates and structure parameters are listed in columns I and II of Table 3. The numbers given in square brackets in these two columns reflect the consistency of the values derived from the different combinations of the moments of inertia.

In view of the data available (Table 2) the seven pairs of atomic coordinates in 2,6-DFP fall into three categories: The first one comprises the five coordinate pairs describing the ring and the hydrogen atom H(4). Substitution coordinates for these five atoms could be calculated independently in the two reference frames. The second category consists of the two equivalent hydrogen atoms H(3) and H(5). These could be placed in the d_4-frame only, since a sample of the D(3)-H(4)-D(5)-species was not available (Section II-1). We therefore had to transform this coordinate pair in order to complete the set of substitution coordinates in the normal reference frame. As both coordinates are large, and since the shift of the centre of gravity for the d_4-species is known to good accuracy, we consider this transformation uncritical. While the two sets of substitution coordinates are thus not completely independent, their interconnection is of little significance for the overall structure determination because the hydrogen atoms are so much lighter than all other atoms in this molecule. The third category of coordinates concerns the fluorine atoms which can not be substituted, and which must therefore be placed by a different method: Since all other atoms have been located through substitution, the determination of the b_F coordinate was readily accomplished from the first moment condition. The conditions $\Sigma m_i a_i = \Sigma m_i a_i b_i = 0$, however do not allow the determination of the a_F coordinate due to the C_{2v}-symmetry of 2,6-DFP. We therefore had to use the observed moment $I_b = \Sigma m_i a_i^2$ to find this last coordinate, taking into account that a complete set of substitution coordinates normally underpredicts the effective moments by a small amount (see, for example, ref. 1 e and 3 b). To quantify this amount for the case of 2,6-DFP we first compared the effective moments I_a^{eff} with the values that resulted from the known b coordinates (row 23 of Table 3). This yielded an average difference of 0.11% and, accordingly, we reduced the effective I_b-values by 0.10% ($\pm 0.05\%$) before calculating the a coordinates of the fluorine atoms.

Inspection of the two sets of results (Table 3, columns I and II) shows that the most poorly determined coordinate is that of the nitrogen atom (row 1) and not, as one would expect, the position of the fluorine atoms (row 7). The large uncertainty in the b_N coordinate arises from the decrease by 0.01 μÅ^2 of I_b for both ^{15}N species (Table 2, row 12, columns I, II and VI, VII), which entails a difference of 0.006 Å in both reference frames between the b_N coordinate calculated from ΔI_a and that calculated from ΔI_c. This, in turn, contributes 90% of the uncertainty of 0.001 Å of the b_F coordinate which is calculated from the first moment condition. The uncertainties in the coordinates $a_{2/6}$ and $a_{3/5}$ are seen to be very small, and the data for the two reference frames agree well with each other. Their contribution to the uncertainty of the a_F coordinate is therefore 10 times smaller than the uncertainty which arises from a possible error by 50% in the estimated difference between $I_b^{\text{effective}}$ and $I_b^{\text{substitution}}$ (row 24 of Table 3).

After the structure parameters of 2,6-DFP had been calculated separately in the two reference frames, the b coordinates obtained in the d_4 frame were transformed to the axis frame of the normal species (shift of centre of gravity by 0.0235 Å). The two sets of substitution coordinates (row 1 – 6 of Table 3) were then merged, and the structure calculation was repeated with the set of averaged substitution coordinates in the manner described above. Inspection of Table 3, column III shows that the deviations (in square brackets) of the averaged coordinates and the resulting structure parameters are comparable, or smaller, than the discrepancies which arise from the use of different combinations of ΔI_g-values in either reference frame. As the set of averaged coordinates is constructed from all experimental data, we are inclined to consider the resulting structure as the best that can be achieved by the substitution method [10].

Finally, the optimised structure of column III was inserted into the least squares fitting programme of internal parameters (GEOM) [11] together with all 33 rotational constants of Table 2. Only the changes in the moments were fitted (LSQ 2), and the results are given in column IV of Table 3. The last column of the table shows the differences between the r_S-cal-

culation and the LSQ-fit of internal parameters. These values indicate neither a serious discrepancy nor a significant improvement of the parameters. We therefore chose the final set of structure parameters so as to be in agreement with the uncertainties emerging from the two different treatments of the isotopic data.

This "best" structure of 2,6-DFP is given in Figure 3, which also contains the corresponding parameters for pyridine [1e].

V. Discussion

The structure determination on 2,6-DFP differs from studies on similar compounds (e.g. refs. 1 and 3) firstly through the observation of all otherwise expensive isotopic species in their natural abundances and, secondly, through the independent determination of the ring structure in two reference frames. While the first point concerns the general feasibility of such studies, the second feature provides proof of the ease with which isotopic species spectra can be identified in DRM spectroscopy. It is also of some significance for the substitution method itself, since the two determinations of the ring structure by the same method reveal the ultimate accuracy that can be expected from this method in comparable molecules. The availability of two independent values for every structure parameter at the same time improves the reliability of the final parameters, and permits uncertainties to be derived from the consistency of two independent results, rather than from the estimated uncertainties of the rotational constants of one set of singly substituted forms. In the case of 2,6-DFP the two structure determinations suggest limits of ± 0.0005 Å and $\pm 0.1^\circ$ for the final bond distances and angles, respectively. This is in quantitative agreement with the findings on other molecules [12] on which we have carried out complete structure determinations with respect to two reference frames.

The structure parameters of 2,6-DFP confirm previous speculations [2e, h, k] about the distortion of the pyridine ring under substitution. Qualitatively, these distortions consist of a shortening of the ring bonds emanating from the carbon atom which carries the substituent. The unsubstituted part of the molecule largely retains the bond distances of pyridine, although the bond angles are noticeably altered. A quantitative comparison of the two structures reveals the following details (compare Figure 3):

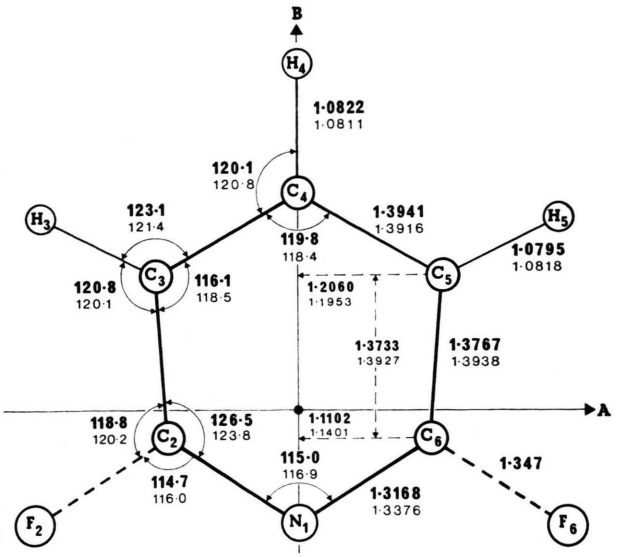

Fig. 3. Structure of 2,6-DFP together with corresponding parameters of pyridine itself (lighter figures).

Corresponding C – H bonds in pyridine and 2,6-DFP differ by 0.002 Å at the most. Since the substitution coordinates of hydrogen atoms normally contain the largest admixture of vibrational effects, the C – H bonds in the two compounds can be considered equal. In contrast, the very slight lengthening (0.0025 Å) of the C(4)-C(3/5) bonds in 2,6-DFP can not be ascribed to the limited accuracy of the substitution method. Along with the extension of this bond, the distance C(3)...C(5) across the ring is increased by 0.021 Å, so that the angles at the C(4) atom (120.1° and 119.8° in 2,6-DFP) approach the pure sp^2-values closer than in pyridine.

Changes from the pyridine geometry in the substituted part of the molecule are about an order of magnitude larger than in the unsubstituted section: The bonds C(3/5) – C(2/6) are contracted by ~ 0.017 Å, and the bonds C(2/6)-N(1) are reduced by ~ 0.021 Å. Due to the latter shortening the distance C(2)...C(6) across the ring is reduced by 2×0.030 Å $= 0.060$ Å. This previously suspected "push in" of the carbon atom carrying the substituent is accompanied by a decrease (1.9°) of the angle C(2)N(1)C(6) to 115.0°. A simultaneous increase (2.7°) of the angles N(1)C(2/6)C(3/5) to 126.5° is compensated by an almost equal decrease (2.4°) of the angles C(2/6)C(3/5)C(4) to 116.1°. The contraction of the substituted section of 2,6-DFP is also reflected in a shortening by ~ 0.019 Å of the

distance between the lines C(3)...C(5) and C(2)...C(6), and a comparable reduction (~ 0.024 Å) of the distance N(1)...C(4) from 2.805 Å in pyridine to 2.781 Å in 2,6-DFP.

The C–F bond length in 2,6-DFP (1.347 ± 0.001 Å) is shorter than that in fluorobenzene (1.354 ± 0.006 Å) (3b), but coincides with that of vinyl fluoride (1.347 ± 0.009 Å) [13], which has been suggested [3b] as the "normal" bond length between fluorine and an sp^2-hybridised carbon atom. The increase to 126.5° of the angle N(1)C(2/6)C(3/5) which results from the "push in" of the C(2/6) atom naturally entails a decrease of the angles F(2/6)C(2/6)C(3/5) or F(2/6)C(2/6)N(1). In 2,6-DFP this decrease is absorbed to equal parts ($\sim 1.4°$) by both exterior angles, and the difference (4.2°) between these angles remains the same as in pyridine. In contrast, the reduction of the angle C(2/6)C(3/5)C(4) by 2.4° is predominantly transfered to the angle C(4)C(3/5)H(3/5) ($+1.7°$), with the angle C(2/6)C(3/5)H(3/5) being increased by 0.7° over the pyridine value.

The stated structural differences between pyridine and 2,6-DFP may be rationalised by similar arguments as those invoked for the structural differences between benzene and fluorobenzene [3b]. However, as these considerations are based on the likely change of the electron distribution (changed hybridisation of the carbon atom C(2/6) on account of the electron withdrawal through fluorine) it appears appropriate to include the values of the quadrupole coupling constants and of the dipole moment in such an analysis. For this reason, a discussion of the chemical implications of the present data is deferred to Part II (Section VI).

Besides the two aspects mentioned above, the present study also differs from work on related compounds [1, 2, 3] through the quick assignment of the spectrum. Just as the observation of ^{13}C and ^{15}N species in natural abundance, and the structure determination with respect to two reference frames, this third distinction also resulted entirely from the use of DRM techniques. Since we have stressed the advantages and explained the details of this approach on various occasions [6e, 14], it is sufficient here to point out that the experimental work on 2,6-DFP was completed within ~ 200 hours. For an evaluation of the human effort and financial expenditure involved in comparable structure determinations by traditional techniques the interested reader is referred to the references.

Acknowledgement

I would like to thank Dr. J. Ladd and Mr. S. Lui (University of Salford) firstly, for the chance to study 2,6-DFP by DRM spectroscopy, secondly, for providing a sample of this compound and, thirdly, for their determined efforts to prepare the two deuterated species required for a complete structure determination. I am deeply indebted to my sister Silvia who relieved me of the chore of typing the manuscript of this paper.

[1] a) K. E. McCulloh and G. F. Pollnow, J. Chem. Phys. **22**, 681 [1954]. — b) B. B. DeMore, W. S. Wilcox, and J. H. Goldstein, J. Chem. Phys. **22**, 876 [1954]. — c) B. Bak, L. Hansen, and J. Rastrup-Andersen, J. Chem. Phys. **22**, 2013 [1954]. — d) B. Bak, L. Hansen-Nygaard, and J. Rastrup-Andersen, J. Mol. Spectrosc. **2**, 361 [1958]. — e) G. O. Sørensen, L. Mahler, and N. Rastrup-Andersen, J. Mol. Struct. **20**, 119 [1974].

[2] a) H. D. Rudolph, H. Dreizler, and H. Seiler, Z. Naturforsch. **22a**, 738 [1967]. — b) H. Dreizler, H. D. Rudolph, and H. Mäder, Z. Naturforsch. **25a**, 25 [1970]. — c) R. A. Kydd and I. M. Mills, J. Mol. Spectrosc. **42**, 320 [1972]. — d) D. Christen, D. Norbury, D. G. Lister, and P. Palmieri, J. C. S. Faraday II, **71**, 438 [1975]. — e) S. D. Sharma, S. Doraiswamy, H. Legell, H. Mäder, and D. Sutter, Z. Naturforsch. **26a**, 1342 [1971]. — f) F. Scappini and A. Guarnieri, Z. Naturforsch. **27a**, 1011 [1972]. — g) W. Caminati and P. Forti, Chem. Phys. Letters **15**, 343 [1972]. — h) S. Doraiswamy and S. D. Sharma, Pramana **2**, 218 [1974]. — i) R. D. Brown, F. R. Burden, and W. Garland, Chem. Phys. Letters **7**, 461 [1970]. — j) S. Doraiswamy and S. D. Sharma, Curr. Sci. India **40**, 398 [1971]. — k) S. D. Sharma and S. Doraiswamy, Curr. Sci. India **41**, 475 [1972].

[3] a) B. Bak, D. Christensen, W. B. Dixon, L. Hansen-Nygaard, and J. Rastrup-Andersen, J. Chem. Phys. **37**, 2027 [1962]. — b) L. Nygaard, I. Bojesen, T. Pedersen, and J. Rastrup-Andersen, J. Mol. Struct. **2**, 209 [1968]. — c) J. Casado, L. Nygaard, and G. O. Sørensen, J. Mol. Struct. **8**, 211 [1971].

[4] a) The present study resulted from an approach by Dr. J. Ladd (University of Salford) for a partial structure determination on 2,6-difluoropyridine. Such information was desirable to facilitate the interpretation of nmr spectra. — b) The preparation of samples will be described by J. Ladd and S. Lui in conjunction with their study of liquid crystals of this compound by pulsed nmr spectroscopy.

[5] a) O. L. Stiefvater, J. Chem. Phys. **62**, 244 [1975]; — b) ibid. **63**, 2560 [1975].

[6] a) R. C. Woods III, A. M. Ronn, and E. B. Wilson, Jr., Rev. Sci. Instrum. **37**, 927 [1966]. — b) O. L. Stiefvater, H. Jones, and J. Sheridan, Spectrochim. Acta **26a**, 825 [1969]. — c) O. L. Stiefvater, Z. Naturforsch. **30a**, 1742 [1975]. Part I. — d) O. L. Stiefvater, Z. Naturforsch. **30a**, 1756 [1975], Part II. — e) O. L. Stiefvater, First Europ. Conf. on Microwave Spectrosc., Bangor 1970, Paper B 1–3. (Also DRM III, to be published.) — f) O. L. Stiefvater, (DRM IV, to be published).

[7] a) R. T. Bailey and T. Steele, Spectrochim. Acta **23 A**, 2997 [1967]. — b) J. H. S. Green, D. J. Harrison, and M. R. Kipps, Spectrochim. Acta **29 A**, 1177 [1973].
[8] P. Nösberger, A. Bauder, and Hs. H. Günthard, Chem. Phys. **1**, 426 [1973] (the LSQ fitting programm was kindly made available by Dr. P. Nösberger).
[9] A list of transition frequencies may be obtained from the author.
[10] a) J. Kraitchman, Amer. J. Phys. **21**, 17 [1953]. —b) C. C. Costain, J. Chem. Phys. **29**, 864 [1964].
[11] P. Nösberger, A. Bauder, and Hs. H. Günthard, Chem. Phys. **1**, 418 [1973] (the computer programme GEOM was kindly made available by Dr. P. Nösberger).
[12] O. L. Stiefvater (to be published).
[13] D. R. Lide, Jr. and D. Christensen, Spectrochim. Acta **17**, 665 [1961].
[14] O. L. Stiefvater, a) 2nd Colloquium on High Resolution Spectroscopy, Dijon, France, 1971 (Lecture C). — b) Fourth Austin Symposium on Gas Phase Molecular Structure, Austin, Texas, 1972 (Paper W6). — c) 3rd Colloquium on High Resolution Spectroscopy, Tours, France, 1973 (Paper C7). — d) Fifth Austin Symposium on Gas Phase Molecular Structure, Austin, Texas, 1974 (Paper M5). — e) 3rd European Microwave Spectroscopy Conference, Venice, Italy, 1974 (Paper C9).